A COMPARATIVE STUDY ON MACHINE LEARNING ALGORITHMS FOR ECG ANOMALY DETECTION

Abstract

Medical data often exhibit class imbalance, where the number of samples in different classes is not proportional. This imbalance can pose significant challenges to traditional classification algorithms. This report explores the application of Support Vector Machines (SVM) to imbalanced ECG classification, discussing the inherent issues, techniques for addressing classification, and experimental results showcasing the effectiveness of SVM in handling ECG datasets.

Authors

Aditi Mohapatra
Department of ETC Engineering,GP
Dhenkanal, Odisha
aditi.pkl.123@gmail.com

I. INTRODUCTION

The World Health Organization (WHO) claims that cardiovascular disease is one of the leading global causes of death. Delay in diagnosis often results in another organ being damaged, which leads to many heart attack victims dying. An electrocardiogram (ECG) is a crucial tool for identifying and diagnosing heart issues in people.The strain on doctors increases daily as the number of cardiac patients rises. In the current research scenario, automation is required to decrease the physical workload through computerized technologies.

In normal conditions, the Sinoatrial (SA) node in the right atrium is the heart's natural pacemaker and begins the heartbeat. Electrical impulses from the SA node propagate across both atria, causing them to depolarize. The P-wave is used to illustrate atrial depolarization. The time it takes for electrical impulses to pass from the SA node to the Atrioventricular (AV) node located near the AV valve is represented by the PQ segment.The AV node acts as an electrical conduit to the ventricles, delaying electrical impulses that cause the atria to relax or repolarize. The QRS complex obscures atrial repolarization. The AV node initiates electrical impulses in the His bundle, which is then divided into right and left bundles branches. These branches send impulses of electricity to the heart's apex. The electrical impulses are subsequently transmitted to the Purkinje fibers and dispersed throughout the myocardium of the ventricular walls, inducing depolarization of the ventricles.The QRS complex is an indicator of ventricular depolarization. The next phase is ventricular contraction, which results in a plateau in the myocardial action potential and is depicted by the ST segment. The T-wave represents ventricular repolarization at this point.

As a result, a normal ECG signal may be divided into the following fiducial points:

- The P-wave represents the depolarization of the atria.
- Q-wave is associated with the deflection immediately preceding ventricular depolarization.
- R-wave is related to the peak of ventricular depolarization.
- S-wave is associated with the deflection following ventricular depolarization.
- T-wave is related to ventricular repolarization.

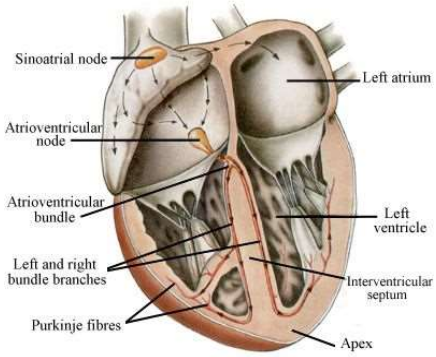

Figure 1: Anatomy of Heart

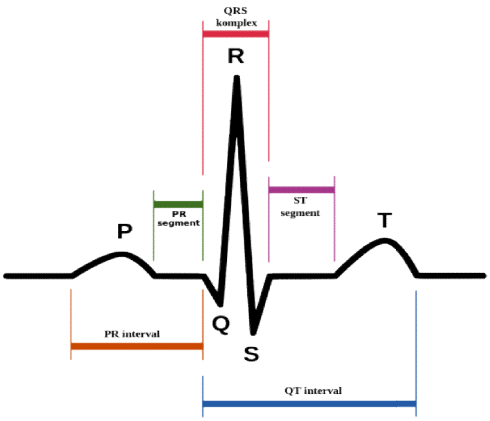

Figure 2: Normal ECG beat.

An ECG gives two types of data: To begin, a doctor can record time intervals on the ECG to determine how long an electrical wave travels through the heart. The amount of time it takes for a wave to go from one portion of the heart to another indicates whether the electrical discharge is normal, slow, rapid, or irregular. Second, a cardiologist can determine whether sections of the heart are too big or overworked by measuring the volume of electrical impulses traveling through the heart muscle.

1. **Atrial Fibrillation (AF):** Arrhythmia is a frequent cardiovascular condition that can develop alone or in combination with other cardiac issues. Atrial fibrillation (AF) is among the most prevalent kind of long-term arrhythmias. Poor coordination of atrial activity in people with AF may reduce the atrioventricular mechanism, increasing the risk of stroke, cardiovascular illness, and mortality [17]. Atrial fibrillation (AF) is a potentially fast heartbeat (arrhythmia) that can lead to heart clots. AF raises the risk of having a heart attack, developing heart failure, or other cardiovascular-related illness.

2. **First-Degree Atrioventricular Block (I-AVB):** AVB I is a condition that causes impulses from the chambers of the cardiac muscle to the the ventricles to be delayed by the AV node. AVB I has been associated to a higher risk of coronary artery disease, atrial fibrillation, and mortality. There is also a larger possibility of more severe AV obstruction [14].

3. **Bundle Branch Block (BBB):** Bundle branch block (BBB) is a common conduction block problem that is often linked with consequences such as hypertrophy of the ventricular walls, pulmonary embolism (PE), and ischemia of the heart. The two basic kinds of BBB are right BBB (RBBB) and left BBB (LBBB), which are triggered by delayed stimulation of either the right and left the ventricles, correspondingly. The BBB can induce partial plasma passage from the atria to the pulmonary artery, lowering heart function efficiency. As a result, for effective therapy, early identification and actual time warning of BBB are critical. The automated ECG method is based on detecting RBBB and LBBB. [18].

4. **Premature atrial contraction (PAC):** PAC occurs when an area other than the atria depolarizes before the SA node, causing a premature beat. The P-wave of the PAC occurs early in the cardiac cycle. Furthermore, the PR interval is reduced, indicating that the beat originated in the atria near the AV node. A compensating pause occurs when the time between the PAC and the following contraction is somewhat longer.

5. **Premature ventricular contraction (PVC):** At times, the electrical signals that control the heart's muscular contractions may be disturbed. While these can occur in healthy people on occasion, some of them may indicate cardiac disease. The most prevalent arrhythmia is improper contraction of the ventricular (PVC).

6. **ST-segment depression (STD):** ST segment alteration is a critical sign of myocardial ischemia, and detecting ST deviation is critical in myocardial infarction diagnosis. ST-segment elevation is more common in individuals with transmural myocardial ischemia or variant angina pectoris. In contrast, ST-segment depression is more common in patients with subendocardial ischemia or stable or unstable angina. The electrocardiogram (ECG) is a non-invasive, easy, low-cost, and frequently used method of detecting ST deviation [11].

   The ST segment in an ECG is defined as the period between the end of the QRS complex and the start of the T wave. To determine a ST segment variation, an initial point of reference must be specified. The J point is the starting point of the segment known as the ST and is used to identify ST segmental deviations by comparing it to the ST-segment change detection reference point[18].

7. **ST-segment elevated (STE):** ECG anomalies in the Q, T, and ST segments are used to identify STE. The Q wave is simple to identify; however, correct assessments of the ST segment must be accompanied by exact extraction from the waveform known as the T wave as well as the J point. Although the amplitude of the T wave in an electrocardiogram (ECG) data is significantly greater than that of the P wave, the T wave is more difficult to extract. Because getting an exact J point is difficult, the ST segment is typically obtained by monitoring a certain limited part immediately following the R-peak (i.e., during a given number of millisecond), when the ST section is more likely to be detected [14].

II. METHODOLOGY

Figure 3 depicts the suggested approach for accurate and automated categorization of ECG data.

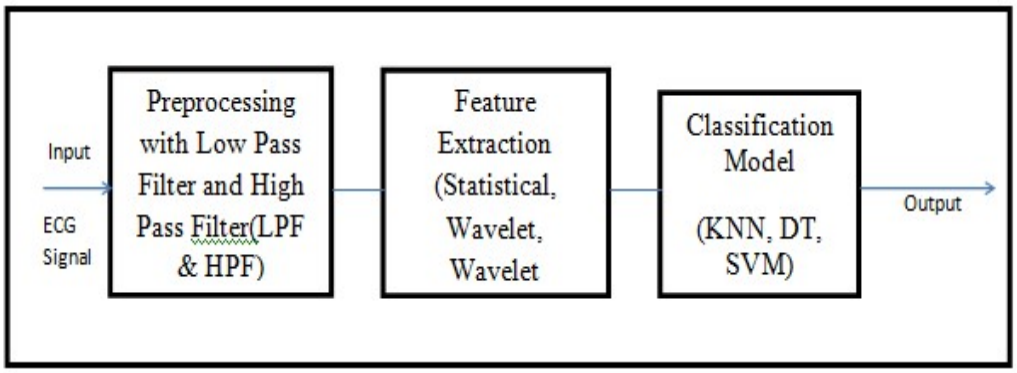

Figure 3: Block diagram of Proposed Methodology

1. **Dataset Description:** The suggested method is validated using the publicly available CPSC2018 challenge dataset [17]. Eleven hospitals provided recordings of challenge ECG data. There are 6,877 points of information in the training set, 3178 of which belong to female and 3699 of which are male. The test set comprises 2,954 ECG recordings ranging in length from 6s to 60s, while the study set possesses twelve leads for ECG recordings spanning in length from 6s to 60s. This dataset is used to detect 12-lead ECG irregularities lasting a few seconds to a few minutes. The CPSC2018, which is used by 12-lead ECGs, has one normal type and eight pathological types.

2. **Preprocessing:** To remove noise, a low-pass filter is utilized the excessive signal in the ECG data. The raw ECG signal is first a bandpass filtered, which separates the core QRS activity concentrated at 10 Hz while attenuating low frequencies related to T waves, background drift, and higher frequencies related to electromyography, or noises and electric line interference. The primary objective is to prevent the information represented by the ECG signal from being lost after it has been filtered out. (1) and (2) depict the various equations for the cascaded LPF and the high-pass filter (HPF). The LPF filter has an 11 Hz cutoff frequency and a six-sample delay, whereas the HPF has a 5 Hz cutoff frequency and a 16-sample delay, respectively. All of the filter coefficients are integers.

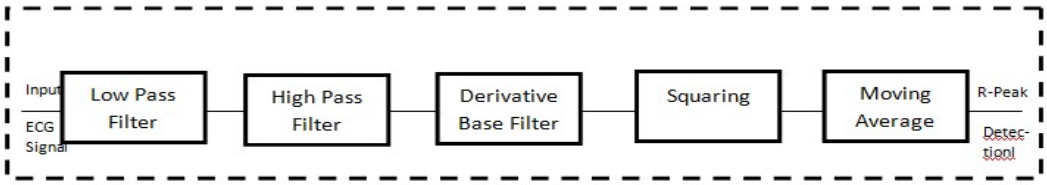

Figure 4: Block Diagram of Pan and Tompkins Algorithm.

- **Low Pass Filter:** The second-order low-pass filter's transfer function is

$$\frac{(1-Z^{-6})^2}{(1-Z^{-1})^2} = H(Z) \quad (1)$$

The amplitude response is

(2)

H (w T) = Sin2 (3wT) / (Sin2Wt/2)

Where T is the sample time, the filter's difference equation is

Y (n T) = 2 y (n T-T) – y (nT-2T) + x (n T) – 2 x (nT6T) + x (nT-12T) (3)

Where the cutoff frequency is around 11Hz and the gain is 36. Six tests are required to process the filter.

- **High Pass Filter :** The purpose of a high- pass filter is to deduct the output from a a second-order low-pass filtering from the outputs of an all-pass filter (that is, to simulate signals within the original signal). This filter's transfer characteristic is

$$\frac{-1+32Z^{-1}\ +Z^{-3}}{1+Z^{-1}} = H(z) \quad (4)$$

The amplitude response is

H(w T)=|H (w T)| = [256+Sin2(16wT)] 1/2 / (cos (Wt/2)) (5)

The difference equation is
Y (n T) = 32 x (n T – 16T) – [y (n T – T) + x (n T) – x (n T –32T)] (6)

This filter has a low cutoff frequency of around 5Hz, a gain of 32, and a delay of 16 samples.

- **Derivative:** After filtering, the signal is separated to supply the QRS complex slop data. We utilize a five-point subsidiary with the exchange function

H (z) = (1/8T) (Z-2 Z-1 - Z1 - Z2) (7)

The Amplitude response is
H (w T) = (1/4T) [sin (2wT) + 2 sin (w T)]. (8)

The difference equation is
Y (n T) = (1/8T) [-x (n T – 2T) – 2x (n T – T) +2 x (n T+T) + x (n T + 2T)]. (9)

- **Squaring:** Squaring After differentiation, the signal is squared point by point. The condition of this operation is

$$Y(n\,T) = [X(n\,T)] \quad (10)$$

This makes all information focused positive and does nonlinear amplification of the yield of the subsidiary emphasizing the higher frequencies (i.e., overwhelmingly the ECG frequencies).

- **Moving Average Window:** Moving Windows Integrate: The purpose of shifting-window integrated is to get spectral information for features as well as the tilt of the R wave. It derives from

$$Y(n\,T) = (1/N)\,[x(n\,T - (N\text{-}1)\,T) + x(n\,T - (N-2)\,T) + \ldots\ldots + x(n\,T)] \quad (11)$$

Graph 2 demonstrates the link between the wavefronts of moving-window integrations and the complex of QRS, where N is the total number of repetitions inside the combined window's breadth. It is critical to have N samples within the moving window. The dimension of the aperture should be roughly equal to the breadth of the greatest conceivable QRS complex. The combination of the waveforms will mix the QRS and T complexes if the window is large enough. In case it is too narrow, a few QRS complexes will produce a few crests within the integration waveform. These can cause trouble in ensuing QRS location forms. The width of the window is decided observationally. For our sample rate of 200 tests/s, the window is 30 tests wide (150 ms).

When compared to others, Pan Tompkins' studies had a significant influence on QRS detection. A review of the literature suggests that this strategy is one of the most important algorithms for finding QRS peaks. The precision of any Electrocardiogram (ECG) waveform extraction is critical in providing a better diagnosis of any heart-related illness.

A typical ECG should have three parts: P wave, QRS complex, and T wave. These waves reflect the action of the heart, such as the P wave produced by muscular compression of the atria, and their duration indicates atrial extension. The Q wave provides the principal negative esteem and is routinely estimated to be 25% smaller than the R wave value. The Pan Tompkins Algorithm block diagram is illustrated in the picture below.

- **Feature Extraction:** To boost machine learning model training, a few preprocessing processes are employed rather of just feeding the data to the classifying model. The mean, median, wavelet, energy entropy, and standard deviation properties are all examined.

- **Mean:** Mean of each input data x_i is calculated as

$$\mu = \frac{1}{N}\sum_{i=0}^{N-1} x_i \quad (12)$$

- **Median:** The median value for signals with an odd amount of sizes is computed as

$$Median = \frac{\left(\frac{N}{2}\right)^{th} term + \left(\frac{N}{2}+1\right)^{th}}{2} \quad (13)$$

The formula that follows is used for data sizes that are odd

$$Median = \frac{N+1}{2} \quad (14)$$

- **Standard Deviation:** Another aspect is standard deviation, which is computed as

$$^2 = \frac{1}{N-1}\sum_{i=0}^{N-1}(x_i - \mu)^2 \quad (15)$$

- **Energy and Entropy:** The input signal's energy and entropy are computed using Eqn. (16) and (17).

$$Energy = -\sum_{-\infty}^{\infty}|x_i|^2 \quad (16)$$

$$H(x) = -\sum_{i-1}^{N} P(x_i) log P(x_i) \quad (17)$$

- **Wavelet:** The statistical features of an output signal in the signal processing process are determined by its amplitude or energy. 'The wavelet model has the benefit of providing frequency information based on scaling characteristic along temporal variation. The decomposed signal is separated into detailed (d_i) and approximation (α_i), high to frequency components at the i[th level] and is provided as equation.

$$X(t) = \alpha_i(p) + \sum_{p=1}^{1} i(p) = \sum_k \alpha_\gamma(i,y)\beta_{j\gamma}(p) + \sum_{p=1}^{1}\sum_k d_{\gamma(i,y)}\sigma_{ik}(p) \quad (18)$$

Where $_{jy}$denotes the nested space's $_i$scaling function, $_{ik}$ is presented as the mother wavelet, and coefficients $_i(p)$approximate the signal $_{i-1}(p)$ as $_i c\omega_{i-1}$. The loss information is calculated throughout the phase of change between the estimate value by $d_i(p) = \alpha_{i-1}(p) - \alpha_i(p)$ uses signal features . Because basic frequency domain details cannot be used to discover information about temporal variations in emotion, the wavelet-like domain may be used to improve performance.

The wavelet feature, in addition to the previously specified statistical features, is used to train the classification model, and the result is also checked.

Using fourier and entropy parameters, we investigated feature hybridization.

- **Classification Models**

➢ **K-Nearest neighbor (KNN):** The kernel neural network (KNN) is a statistical framework that utilizes a non-parametric in neural network classifier constructed without the use of parameters. It is a quick search approach that finds the closest pattern of training in the characteristic vector space. KNN use iterative computation to get classification results. Two properties, 'K' and the 'distance metric,' are required for more discriminant classification using KNN: K and the distance metric. Throughout the program, the value of 'K' is a constant that is user-defined [24]. K is set to 3 in this approach, and the Euclidean distance metric is investigated.

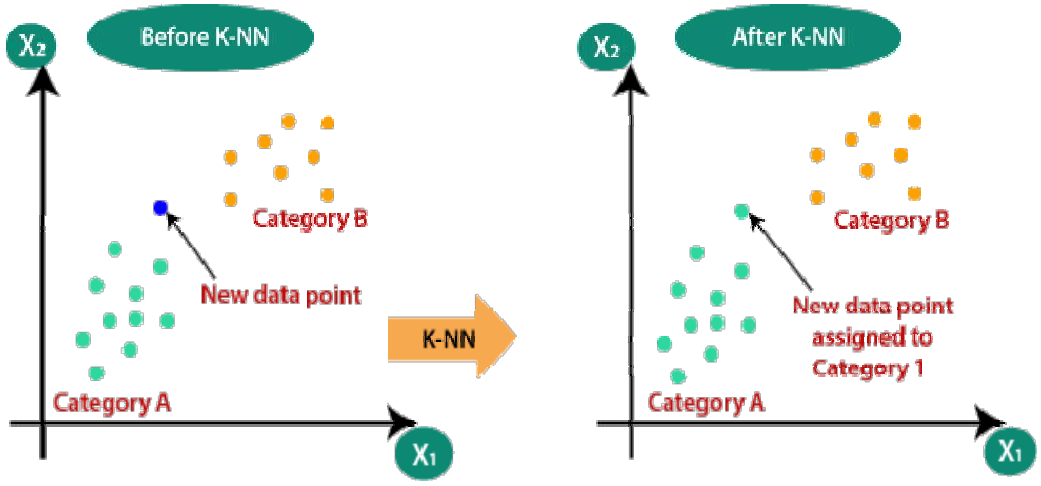

[**Figure 5:** identify the class of a particular dataset]

Assume we have a new data point that has to be assigned to a category. Consider the following image:

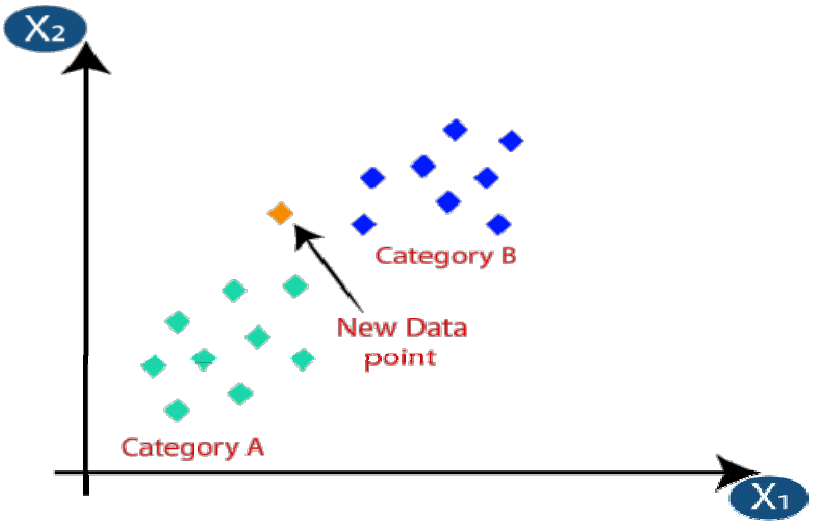

[**Figure 6:** New data point of dataset]

First, we will select the number of neighbors. The Euclidean distance between the data points will then be calculated. The Euclidean distance is the distance between two previously studied locations in geometry. It may be computed as follows:

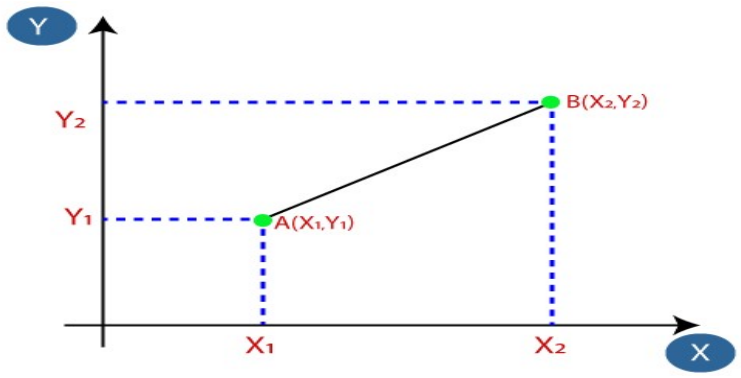

[**Figure 7:** Euclidean distance]

Euclidean Distance between A_1 and $B_2 = \sqrt{(X_2 - X_1)^2 + (Y_2 - Y_1)^2}$ (19)

- **Decision Tree:** The decision tree is a fundamental classification strategy that is used in data mining, expert systems, medical evaluation, satellite images, and other disciplines. They simplify a complicated process by breaking it down into clearly comprehensible predicted making decisions components. In DT, feature nodules are linked to several subnodes or subtrees, as well as decision leaves designated as groupings or classes. A testing nodule produces results based on the value of an immediate characteristic, with each result connected with a set of subtrees. The root node makes it easier to categorize all instances. If the discovered node is a test branch with a suitable subtree, the leaf can help determine the class label of the instance. In this inquiry, a binary tree of choices is employed. Figure 8 depicts a block diagram of the various nodes.

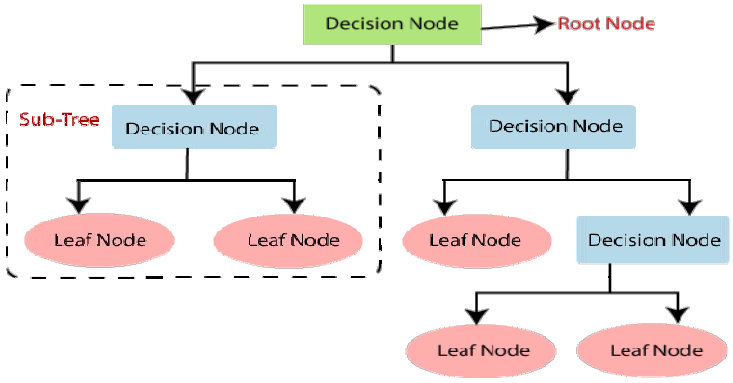

[**Figure 8:** The general structure of a decision tree]

Entropy in the DT model is calculated as follows:

$$E(S) = \sum_{i=1}^{C} -\mathrm{P_i} \log_2 \mathrm{P_i} \quad (20)$$

Entropy for multiple attributes is calculated as

$$E(T, X) = \sum_{c \epsilon x} P(C) E(C) \quad (21)$$

Information gain is the essential requirement of the DT model, and it is calculated as follows:

Information Gain = Entropy(T)-Entropy (T, X)

$$\text{Gini} = 1 - \sum_{i=1}^{C} (P_i)^2 \quad (22)$$

The decision tree contains numerous layers, making it challenging. It may suffer from overfitting, which the Support Vector Machine approach may alleviate. The computing complexity of the decision tree may increase as the number of class labels grows.

- **Support Vector Machine:** SVM is a popular machine learning model that does well with binary data classification. Earlier survey established statistical aspects of a signal, and performance evaluation was reported in previous publications. [18-19] describe how to use a neural network and SVM to create a new classifier. Feature combination may increase the quantity of accessible information about an emotion if the chosen features provide complementary information that is essential for effective hybridization.

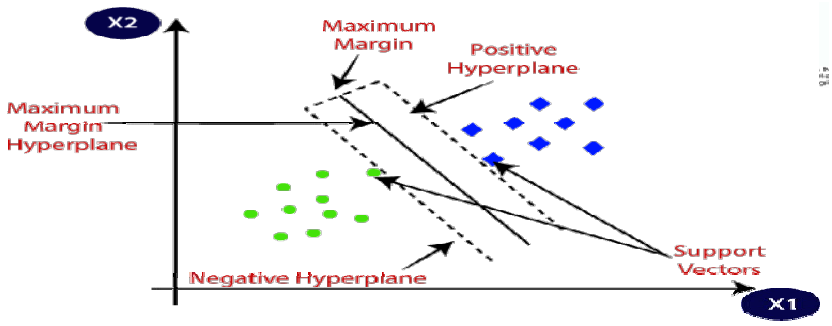

Figure 9: The general structure of a Support Vector Machine

It employs the structure-based mitigation strategy to define an option threshold or the hyperplane for splitting samples into different groups. Consider the practice set $\{(x_m, d_m)_{m-1}^N$ for the SVM classifier. The input characteristic is conveyed by $x_m$and, and the target is d_m. In the hyperplane, these input characteristics will be processed and can be expressed through

$$tx+ C =0 \quad (23)$$

In the Support Vector Machine model, separation of classes is symbolized by

$$t + C \geq 0 \quad \text{for } d_j = 0 \quad (24)$$

$$t + C \leq 0 \quad \text{for } d_j = 1 \quad (25)$$

where t is the weight vector. The bias is symbolized by the letter c. The proposed linear classification problem is solved by maximising the decision boundaries in the hyperspace [24, 25]. It is symbolized by

$$\sum_{m=1}^{N} \omega_m^* \emptyset_m(x) + d \quad (26)$$

where $\emptyset(.)$is the mapping function. The final output $d(x)$ of the SVM classifier is represented by,

$$d(x) = \sum_{j=1}^{N} k(x_{j,}, x) \quad (27)$$

where $k(x_j, x)$ The kernel function. The learning rate of the SVM is considered to be 0.001.

III. RESULTS AND SIMULATIONS

In this work, we have considered the cardiac signal detection. The data is collected from CPSC2018[17]. The data are of one normal and eight different abnormal conditions. The normal and the abnormal signals are shown in Figure 10 through Figure 18 The abnormalities are AF, I-AVB, LBBB.RB, PVC, PAC, STD, and STE are shown below, respectively. Here, the number of samples is 4500.

1. Normal and abnormal signals:

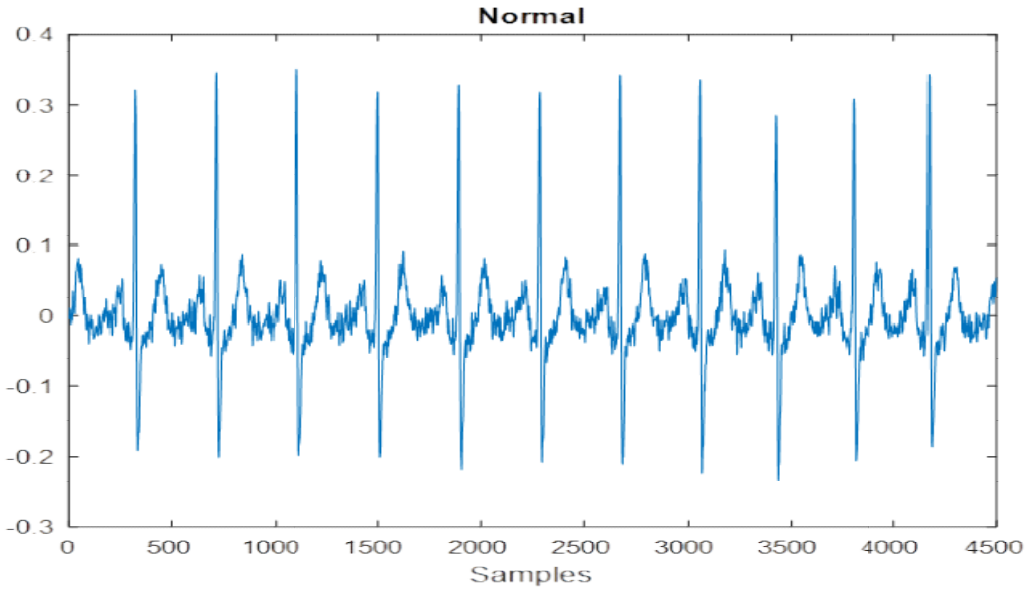

[**Figure 10:** Normal ECG signal]

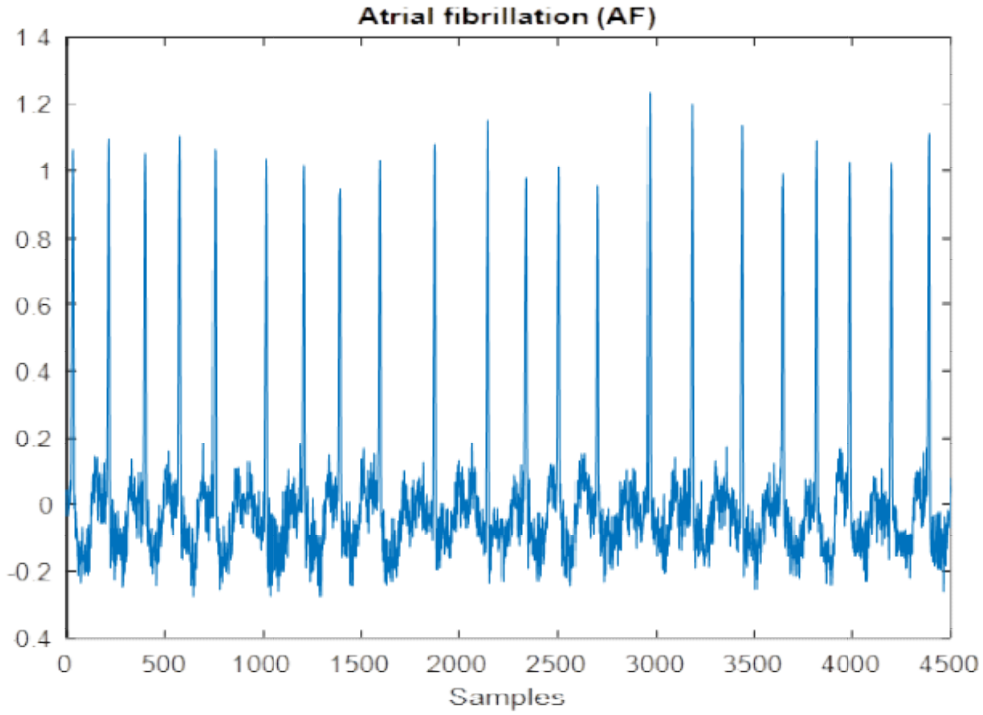

[**Figure 11:** Atrial fibrillation (AF)]

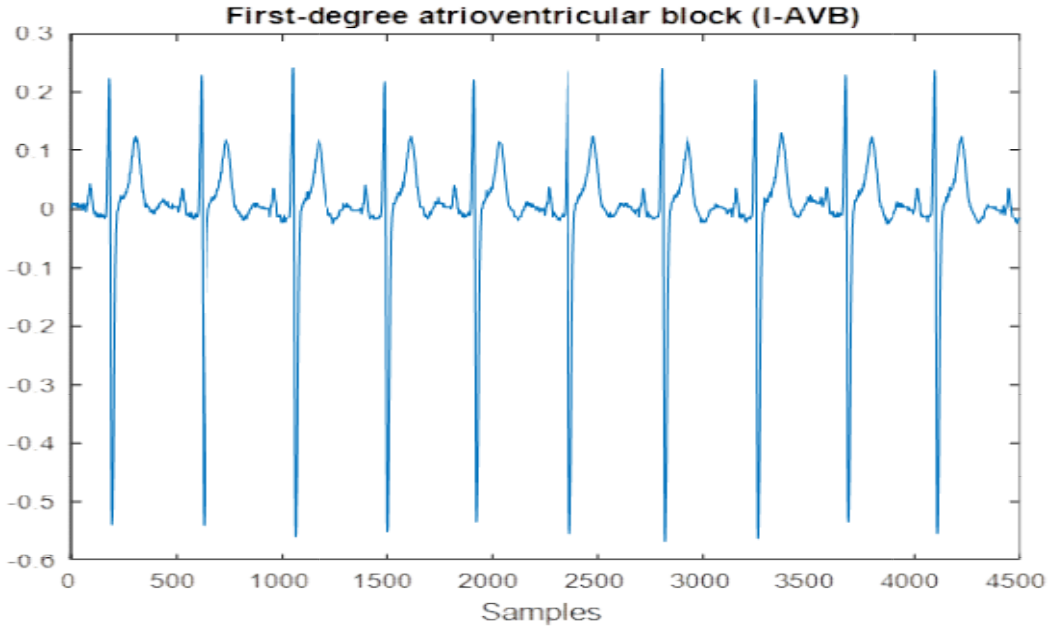

[**Figure 12:** First-degree Atrioventricular Block]

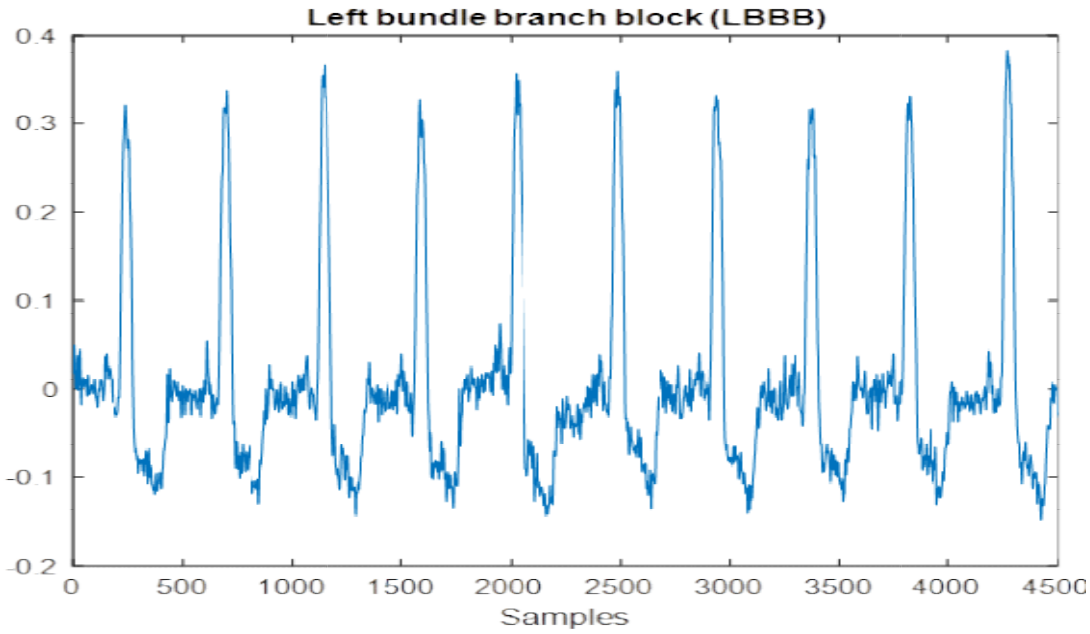

[**Figure 13:** Left bundle branch block (LBBB)]

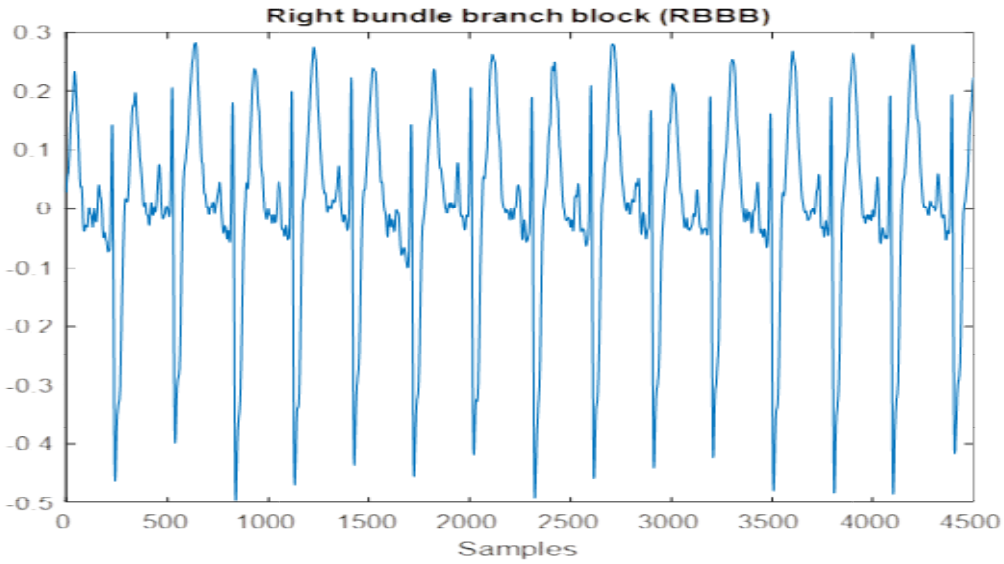

[**Figure 14:** Right bundle branch block (RBBB)]

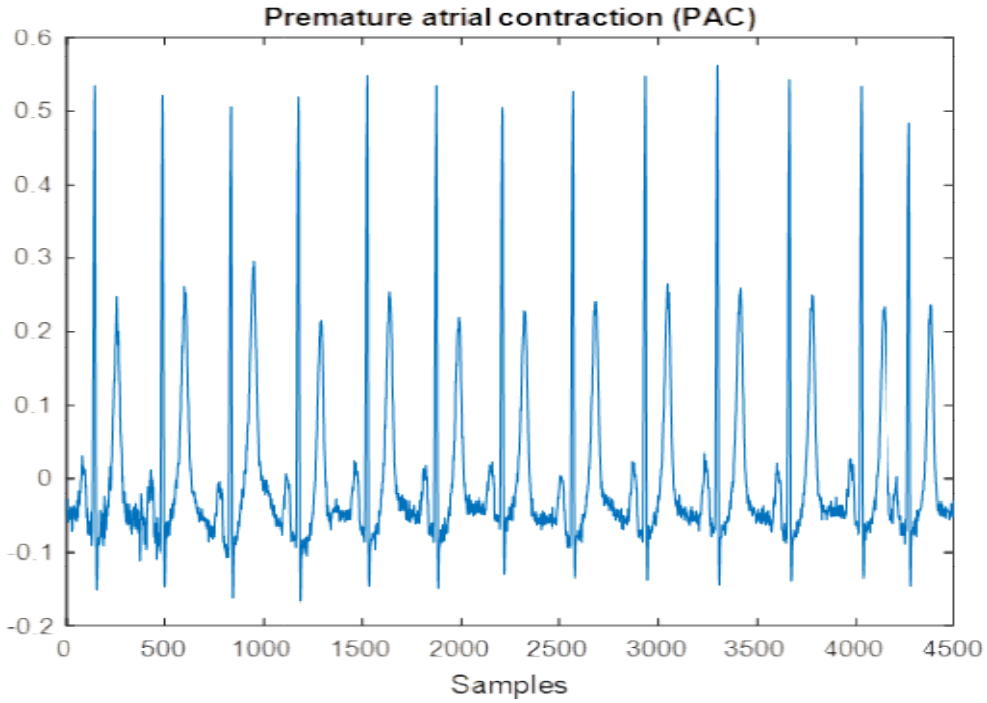

[**Figure 15:** Premature atrial contraction (PAC)]

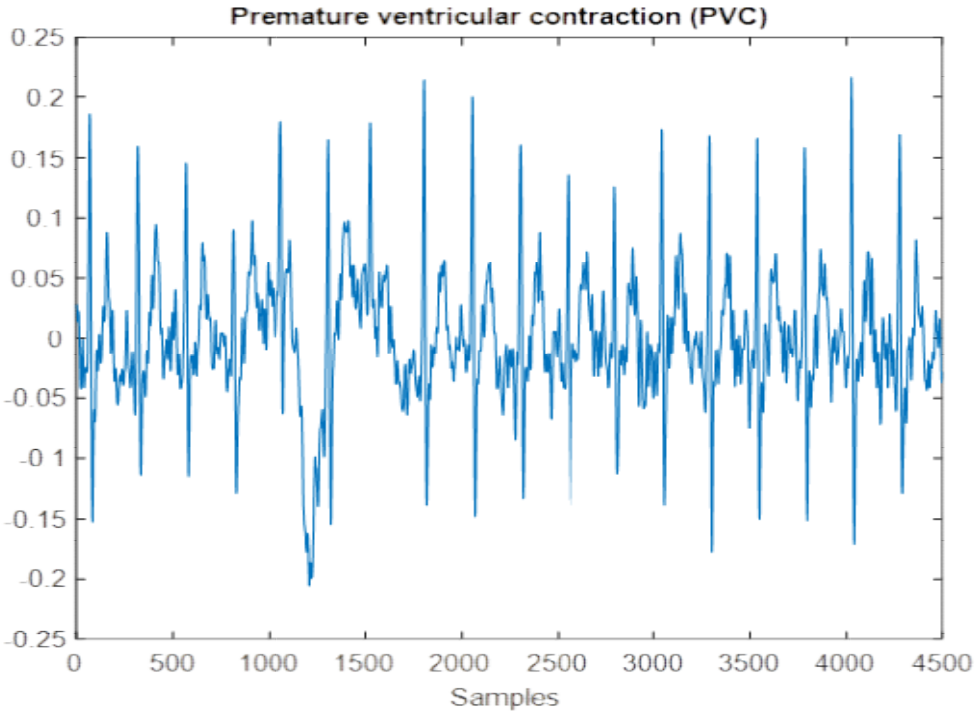

[**Figure 16:** Premature ventricular contraction]

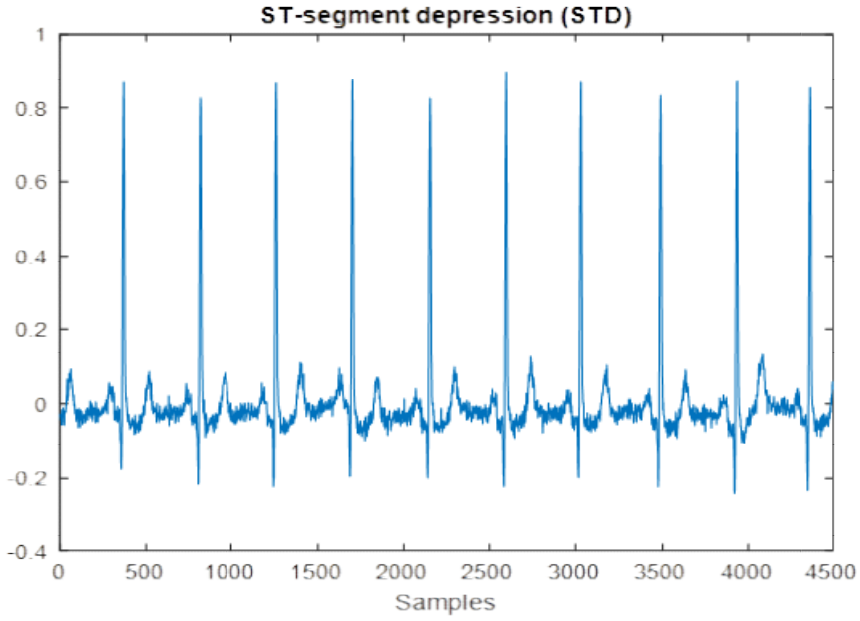

[**Figure 17:** ST-segment depression]

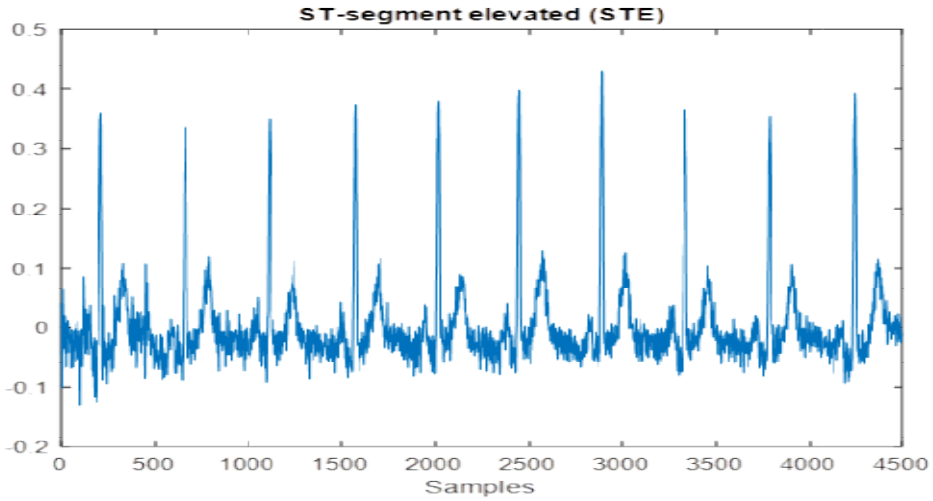

[**Figure 18:** ST-segment elevated signal]

2. **Feature Extraction Result:** As the sample size is larger, The extracted features of the input ECG signals include mean, median, standard deviation, energy, and entropy. Figures 19 to 23 provide histogram charts for the features under evaluation. These features are helpful for the model to detect abnormal signals. For comparison, these features are used in three different classifiers, KNN, DT, and SVM. However, the hybridization of features provides better results than the individual feature use.

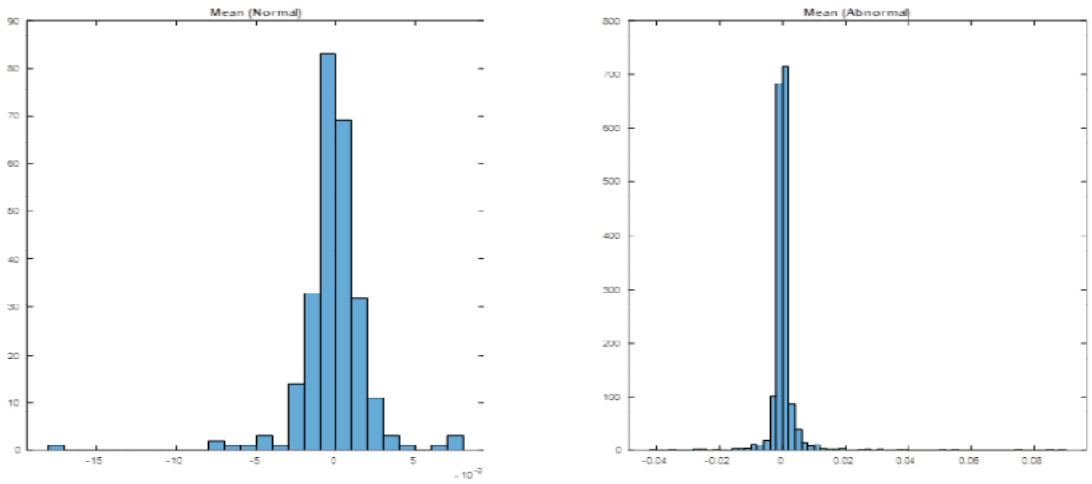

[**Figure 19:** Histogram of the mean of normal and abnormal signals]

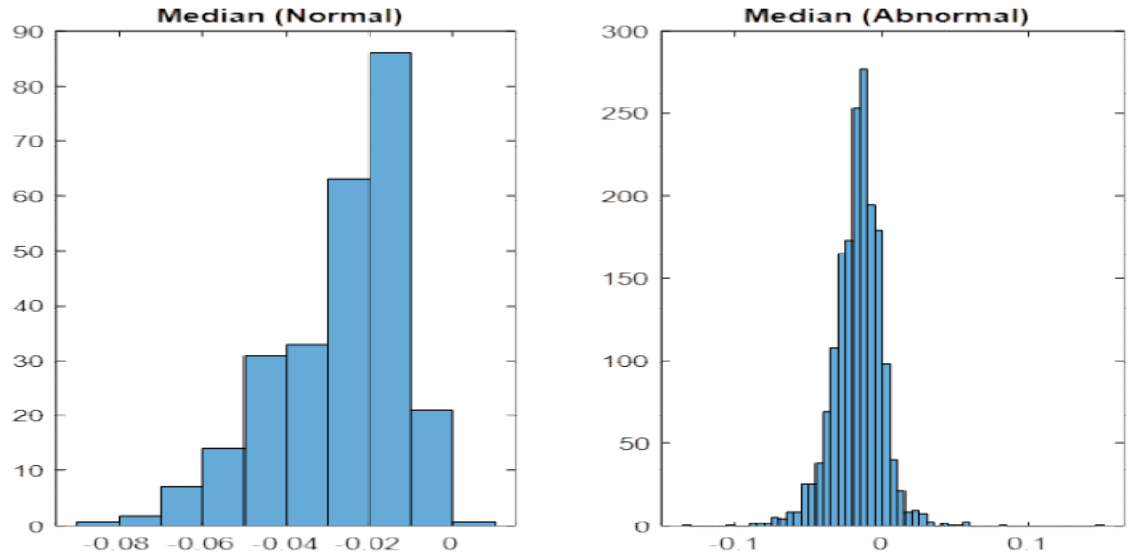

[**Figure 20:** Histogram of the median of normal and abnormal signals]

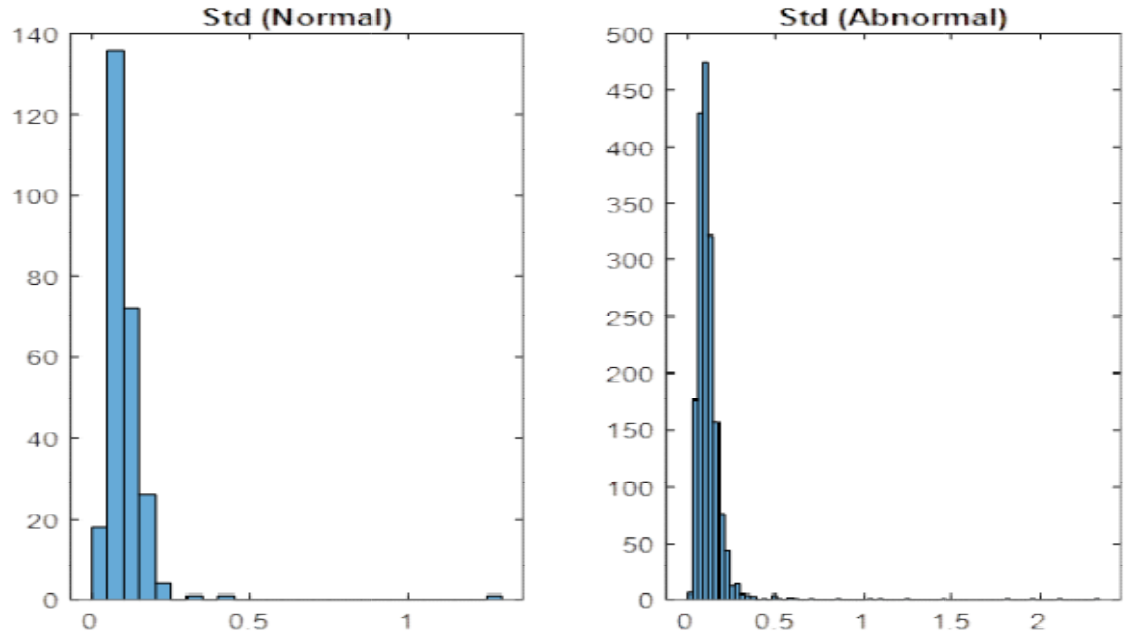

[**Figure 21:** Histogram of the standard deviation of normal and abnormal signals]

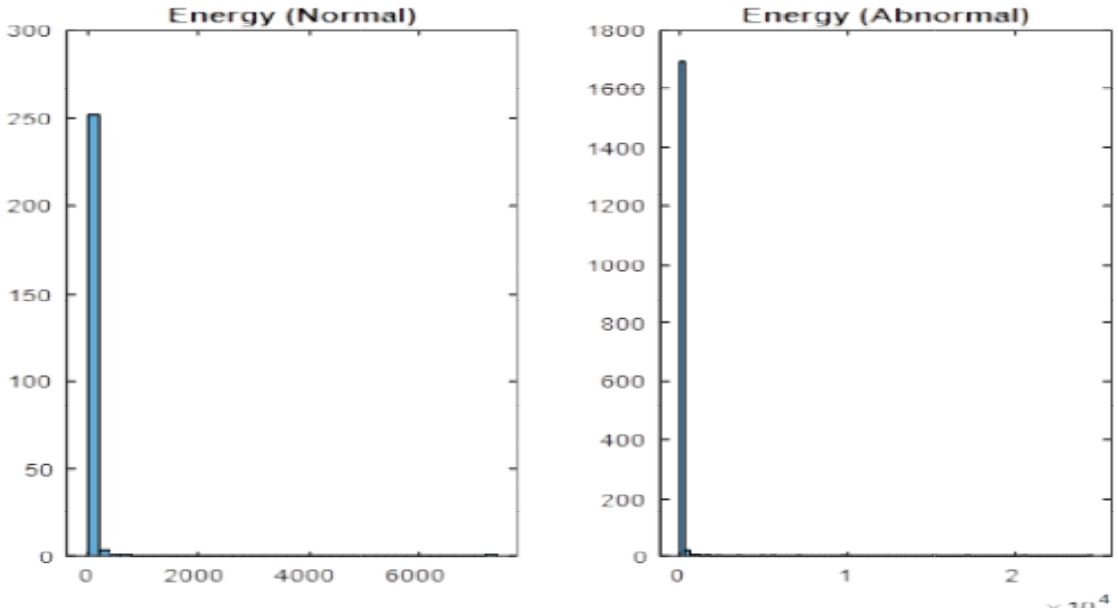

[**Figure 22:** Histogram of energy of normal and abnormal signals]

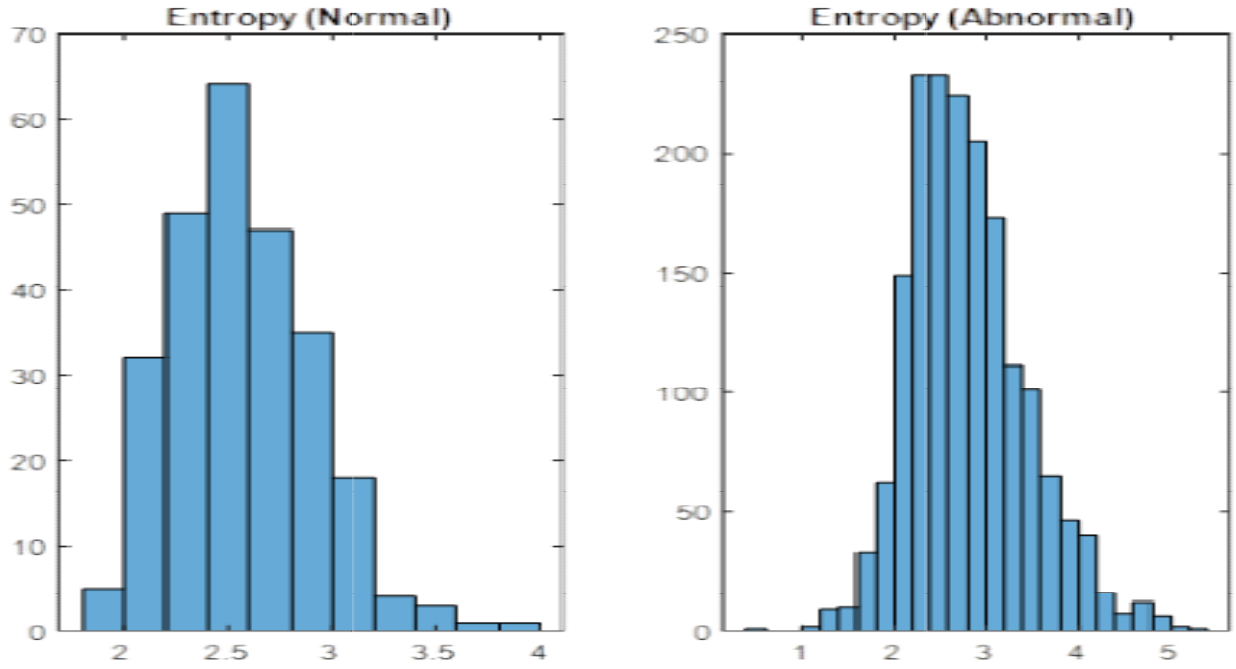

[**Figure 23:** Histogram of entropy of normal and abnormal signals]

Performance Evaluation

3. **Classification Result**: The inputs from the data set are transmitted immediately into machines training classifiers for verification. The efficiency of KNN, DT, and SVM is examined. Table I shows the categorization results from various models. It can observed that the training accuracies are 68.3%,71.22%, and 76.54%, respectively. From the testing point of view, the testing accuracy becomes 78.07% and 80.42%.87%, respectively.

Table 1: Performance of the considered classifiers

	Training	**Testing**						
Classifier	**ACC %**	**ACC %**	**Sens %**	**Spec %**	**Prec %**	**Rec %**	**F-Score %**	**G-Mean %**
KNN	68.3	78.07	16.48	87.27	16.21	16.48	16.34	37.92
DT	71.22	80.42	30.93	87.77	27.31	30.93	29.01	52.11
SVM	76.544	87	75.93	100	57.21	68.41	86.12	67.1

From this table, it is found that the testing accuracy is better than the training accuracy. However, the training accuracy needs to be improved so the features are compared and combined accordingly. The features combination of wavelet and entropy formed better in the Support Vector Machine model as better training and testing accuracy are shown in Table II.

Table 2: SVM performance with varied characteristics

Feature-based	**Classifiers**	**Training**	**Testing**
Statistical	SVM	95.3	91.67
Wavelet	SVM	96.1	92
Proposed Wavelet Entropy	SVM	98.2	96.01

Table III shows a well-observed effectiveness comparison between the suggested approach with current works performed in the discipline of abnormalities identification using ECG data.

Table 3: Comparison of the suggested model to cutting-edge models

Works	Method	Accuracy%
Gad *et al.* [20]	DSNT + SVM	92.16
Amna *et al.* [21]	ESBMM + CNN	93.58
Liu *et al.* [22]	CNN + LRSVM	95.63
Li *et al.* [23]	WPE + RF	95.63
Amna *et al.* [24]	ESBMM + CNN	93.58
Osowski *et al.* [25]	HOS features	94.26
Kamath [26]	Teager energy function features	95.0
Fei [27]	Time intervals features	95.65
Ayar and Sabamoniri [28]	Genetic algorithm	86.96
Proposed Wavelet Entropy method	SVM	96.1%

Any irregularity in brain impulses that can be recognized accurately and automatically can save a person's life. This work applies a machine learning approach with increased characteristics to detect anomalies in ECG data. To determine the optimal model, the performance of three neural network models, KNN, DT, and SVM, is evaluated. SVM demonstrated to be a superior model over the other two. Integrating feature extraction procedures improves SVM efficiency, and it is revealed that SVM works more effectively when taught with the recommended wavelet amplitude parameters. Test results indicate that 96.1% is achieved, which is comparable to cutting-edge processes. In the future, the performance will be enhanced with more characteristics, and the use of deep learning models for verification will be examined.

IV. CONCLUSION

Support Vector Machines offer a promising approach to dealing with imbalanced medical data classification. By utilizing proper techniques such as cost-sensitive learning, resampling, and synthetic data generation, SVM can mitigate the challenges posed by class imbalance, leading to improved classification performance .Future research could explore the combination of SVM with advanced techniques like ensemble learning or deep learning architectures to enhance the handling of imbalanced medical datasets further.

REFERENCE

[1] VijayaArjunan, R. (2016). ECG signal classification based on statistical features with SVM classification. Int. J. Adv. Sig. Img. Sci, 2(1).
[2] Smíšek, R., Hejč, J., Ronzhina, M., Němcová, A., Maršánová, L., Chmelík, J., ...&Vítek, M. (2017, September). SVM based ECG classification using rhythm and morphology features, cluster analysis and multilevel noise estimation. In 2017 Computing in Cardiology (CinC) (pp. 1-4). IEEE.
[3] Sahoo, S., Subudhi, A., Dash, M., &Sabut, S. (2020). Automatic classification of cardiac arrhythmias based on hybrid features and decision tree algorithm. International Journal of Automation and Computing, 17(4), 551-561
[4] Latif, G., Al Anezi, F. Y., Zikria, M., &Alghazo, J. (2020, January). EEG-ECG Signals Classification for Arrhythmia Detection using Decision Trees. In 2020 Fourth International Conference on Inventive Systems and Control (ICISC) (pp. 192-196). IEEE.
[5] Ramkumar, M., Mathankumar, M., &Manjunathan, A. (2020). Classification of Electrocardiogram Cardiac Arrhythmia Signals Using Genetic Algorithm-Support Vector Machines. Bioscience Biotechnology Research Communications (BBRC), Special Issue, 13(11), 138-146.
[6] [6] Padilla-Navarro, C., del Rosario Baltazar-Flores, M., Cuesta-Frau, D., Garza, A. A., & Rodríguez, V. M. Z. (2013, July). Cardiac Arrhythmia Classification Using KNN and Naive Bayes Classifiers Optimized with Differential Evolution (DE) and Particle Swarm Optimization (PSO). In Intelligent Environments (Workshops) (pp. 36-46).
[7] Kasar, S. L., & Joshi, M. S. (2016). Analysis of multi-lead ECG signals using decision tree algorithms. International Journal of Computer Applications, 134(16).
[8] Alarsan, F. I., &Younes, M. (2019). Analysis and classification of heart diseases using heartbeat features and machine learning algorithms. Journal of Big Data, 6(1), 1-15.
[9] Smisek, R., Viscor, I., Evora, A., Bulova, V., Marinova, L., Nejedly, P.,&Plesinger, F. (2021, September). Wavelet Transform Based Detection of the First-Degree Atrioventricular Block. In 2021 Computing in Cardiology (CinC) (Vol. 48, pp. 1-4). IEEE.
[10] Mostayed, A., Luo, J., Shu, X., & Wee, W. (2018). Classification of 12-lead ECG signals with bi-directional LSTM network. arXiv preprint arXiv:1811.02090.
[11] Clark, N., Sandor, E., Walden, C., Ahn, I. S., & Lu, Y. (2018, August). A wearable ECG monitoring system for real-time arrhythmia detection. In 2018 IEEE 61st International Midwest Symposium on Circuits and Systems (MWSCAS) (pp. 787-790). IEEE.
[12] Abubakar, S. M., Saadeh, W., &Altaf, M. A. B. (2018, March). A wearable long-term single-lead ECG processor for early detection of cardiac arrhythmia. In 2018 Design, Automation & Test in Europe Conference & Exhibition (DATE) (pp. 961-966). IEEE.
[13] Liu, F., Liu, C., Zhao, L., Zhang, X., Wu, X., Xu, X., ...& Yin Kwee, E. N. (2018). An open-access database for evaluating the algorithms of electrocardiogram rhythm and morphology abnormality detection. Journal of Medical Imaging and Health Informatics, 8(7), 1368-1373.
[14] Hu, J., Zhao, W., Jia, D., Yan, C., Wang, H., Li, Z., & You, T. (2019, July). A novel detection method of bundle branch block from multi-lead ECG. In 2019 41st Annual International Conference of the IEEE Engineering in Medicine and Biology Society (EMBC) (pp. 79-82). IEEE.
[15] Palo HK, Mohanty MN, Chandra M. Efficient feature combination techniques for emotional speech classification. Int J Speech Technol 2016; 19:135–50. pp. 167–175, 2018. DOI: 10.1016/j.imu.2018.06.002.
[16] M. M. A. Gad, “Feature extraction of electrocardiogram signals using discrete sinc transform,” in 2016 9th Biomedical Engineering International Conference (BMEiCON), pp. 1–4, LuangPrabang, Laos, 2016.
[17] A. Nasim, A. Sbrollini, M. Morettini, and L. Burattini, “Extended segmented beat modulation method for cardiac beat classification and electrocardiogram denoising,” Electronics, vol. 9, no. 7, p. 1178, 2020.
[18] J. Liu, S. Song, G. Sun, and Y. Fu, “Classification of ECG arrhythmia using CNN, SVM and LDA,” Artificial Intelligence and Security., pp. 191–201, 2019.
[19] T. Li and M. Zhou, “ECG classification using wavelet packet entropy and random forests,” Entropy, vol. 18, no. 8, article e18080285, p. 285, 2016.
[20] A. Nasim, A. Sbrollini, M. Morettini, and L. Burattini“Extended segmented beat modulation method for cardiac beat classification and electrocardiogram denoising,” Electronics, vol. 9, no. 7, p. 1178, 2020.
[21] S. Osowski, L. T. Hoai, T. Markiewicz. Support vector ma-chine-based expert system for reliable heartbeat recognition. IEEE Transactions on Biomedical Engineering, vol. 51, no. 4, pp. 582–589, 2004. DOI: 10.1109/TBME.2004. 824138.

[22] C. Kamath, "ECG beat categorization utilising characteristics taken from Teager energy functions in time and frequency domains." 2011's IET Signal Processing, volume 5, issue 6, pages 575–581. DOI: 10.1049/iet-spr.2010.0138

[23] S. W. Fei. Diagnostic investigation on arrhythmia cordis based on support vector machine-based particle swarm optimization. Expert Systems with Applications, 2010, pp. 6748–6752, vol. 37, no. 10.1016/j.eswa.2010.02.126 is the DOI.

[24] S. Sabamoniri and M. Ayar, "An ECG-based feature selection and heartbeat classification model employing a hybrid heuristic algorithm," Information systems in Medicine Unleashed, vol. 13, pp-167-175, 2018.

